The rhinovirus type 14 genome contains an internally located RNA structure that is required for viral replication

K. L. McKnight and S. M. Lemon

RNA 1998 4: 1569-1584

RNA (1998), *4*:1569–1584. Cambridge University Press. Printed in the USA.

The rhinovirus type 14 genome contains an internally located RNA structure that is required for viral replication

KEVIN L. MCKNIGHT and STANLEY M. LEMON

Department of Microbiology and Immunology, The University of Texas Medical Branch at Galveston, Galveston, Texas 77555-1019, USA

ABSTRACT

***Cis*-acting RNA signals are required for replication of positive-strand viruses such as the picornaviruses. Although these generally have been mapped to the 5′ and/or 3′ termini of the viral genome, RNAs derived from human rhinovirus type 14 are unable to replicate unless they contain an internal *cis*-acting replication element (*cre*) located within the genome segment encoding the capsid proteins. Here, we show that the essential *cre* sequence is 83–96 nt in length and located between nt 2318–2413 of the genome. Using dicistronic RNAs in which translation of the P1 and P2–P3 segments of the polyprotein were functionally dissociated, we further demonstrate that translation of the *cre* sequence is not required for RNA replication. Thus, although it is located within a protein-coding segment of the genome, the *cre* functions as an RNA entity. Computer folds suggested that *cre* sequences could form a stable structure in either positive- or minus-strand RNA. However, an analysis of mutant RNAs containing multiple covariant and non-covariant nucleotide substitutions within these putative structures demonstrated that only the predicted positive-strand structure is essential for efficient RNA replication. The absence of detectable minus-strand synthesis from RNAs that lack the *cre* suggests that the *cre* is required for initiation of minus-strand RNA synthesis. Since a lethal 3′ noncoding region mutation could be partially rescued by a compensating mutation within the *cre*, the *cre* appears to participate in a long-range RNA–RNA interaction required for this process. These data provide novel insight into the mechanisms of replication of a positive-strand RNA virus, as they define the involvement of an internally located RNA structure in the recognition of viral RNA by the viral replicase complex. Since internally located RNA replication signals have been shown to exist in several other positive-strand RNA virus families, these observations are potentially relevant to a wide array of related viruses.**

Keywords: *cis*-acting RNA replication element; replicons; rhinovirus; RNA replication

INTRODUCTION

Widely disparate families of positive-strand RNA viruses appear to share similar genome replication strategies. The replicative (nonstructural) proteins encoded by these viruses contain several conserved domains, suggesting that these proteins, in concert with host cell components, support similar mechanisms for RNA replication (Hodgman, 1988). A poorly understood but critically important feature of the replication cycle is that RNA transcription is confined specifically to viral sequences, and does not result in amplification of cellular messenger RNAs. It is generally believed that the specificity of genome amplification results from interactions of the respective replicase complexes with unique *cis*-acting RNA structures located at both 5′ and 3′ termini of the viral RNA (Pogue et al., 1994). Once fully assembled, the replicase complex appears to direct replication via a mechanism common to all positive-strand RNA viruses. The input positive-strand RNA is transcribed to form complementary minus-strands that in turn serve as a template for progeny genomes in a nonconservative series of reactions. Striking differences exist, however, in the nature of the terminally positioned *cis*-acting RNA structures involved in replication (Pogue et al., 1994).

The human rhinoviruses are small, nonenveloped positive-strand RNA viruses that are classified within a separate genus of the family *Picornaviridae*. The positive-strand genome of one of these viruses, human rhinovirus type 14 (HRV-14), is 7,212 nt in length, 3′ polyadenylated, and functions directly as mRNA after

Reprint requests to: Stanley M. Lemon, Department of Microbiology and Immunology, The University of Texas Medical Branch at Galveston, 301 University Boulevard, Galveston, Texas 77555-1019, USA; e-mail: smlemon@utmb.edu.

being released into the cytoplasm of host cells within the respiratory epithelia (for a review of rhinovirus infections, see Gwaltney, 1995). HRV-14, like all picornaviruses, expresses its genetic information in the form of a single, large polyprotein. This polyprotein is divided functionally into a P1 segment that includes 4 capsid proteins, and the P2 and P3 segments that comprise the nonstructural proteins involved in RNA replication, as well as the small, genome-linked protein VPg (3B) (see Fig. 1). The polyprotein is proteolytically processed into at least 11 functional proteins by two virally encoded proteinases. Primary cleavage of the polyprotein occurs between P1 and P2 under direction of a *cis*-acting viral proteinase ($2A^{pro}$), whereas almost all other polyprotein cleavage events are mediated by the *cis* or *trans* activities of a second proteinase $3C^{pro}$ (or $3CD^{pro}$).

Although much has been learned about these processes, a coherent understanding of the mechanism for replication of picornaviral RNA remains lacking (for a review of picornavirus replication, see Wimmer et al., 1993). Available evidence indicates that the input RNA is first copied into the minus-strand form in a primer-dependent reaction initiated at the 3′ end of the genome. This occurs in association with membranous structures formed by a reordering of host cellular membranes, a process mediated by the nonstructural proteins of the virus (Bienz et al., 1990). Completion of the minus strand then leads to reinitiation of transcription at the 3′ end of the minus strand to produce new positive-stranded, progeny RNA molecules (Andino et al., 1993). Thus, replicative intermediates include both negative- and many nascent positive-strand copies. While there has been some controversy over the primer-dependent nature of picornavirus RNA polymerases, the primer for the minus-strand RNA replicase for poliovirus has recently been determined to be the VPg protein (Paul et al., 1998).

The 5′ and 3′ nontranslated termini of picornaviral RNAs have been considered to possess all of the *cis*-acting signal(s) required by the viral RNA replicase to initiate transcription (Xiang et al., 1997). All replication-competent, subgenomic picornavirus RNAs, whether naturally derived or artificially constructed, contain both the 5′ and 3′ terminal sequences of the wild-type genome (Cole, 1975; Kajigaya et al., 1985; Kuge et al.,

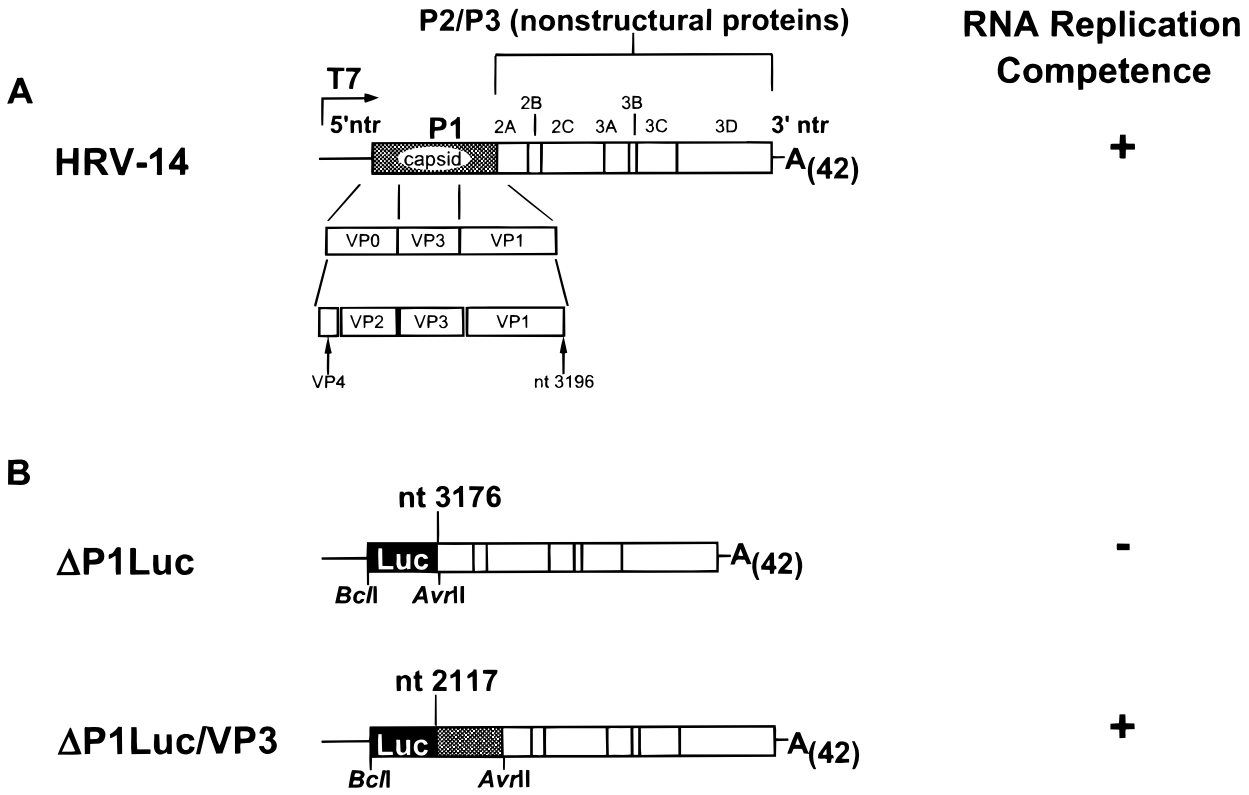

FIGURE 1. The infectious cDNA clone of HRV-14, pWR3.26, and candidate replicon constructs. **A**: A schematic diagram of the polyprotein and protein processing scheme for HRV-14 which can be rescued following transfection of pWR3.26 RNA transcripts (Lee et al., 1993). P1 is the precursor of the capsid proteins; P2 and P3 are precursors of the nonstructural proteins. The capsid precursor is processed into four proteins: VP4, VP2, VP3, and VP1. **B**: The candidate replicon RNAs that contain the luciferase coding sequence (solid sequence), ΔP1Luc and ΔP1Luc/VP3, the construction of which has been described previously. Note (at right) that the insertion of a downstream segment of the P1 region (cross-hatched segment) is required for efficient replication of these HRV-14 replicon RNAs (McKnight & Lemon, 1996). Luc: luciferase coding sequence.

1986; Kaplan & Racaniello, 1988; Choi et al., 1991; Percy et al., 1992; McKnight & Lemon, 1996). In addition, synthetic replication-competent subgenomic poliovirus RNAs have been constructed that contain little or no P1 coding sequence. These RNAs need only express functional forms of the P2 and P3 proteins to direct their replication (Andino et al., 1993; Porter et al., 1995). However, we reported previously that a cis-acting replication element (*cre*) located within a 1-kb segment of the P1 region (nt 2117 and 3196) of the HRV-14 genome is required for efficient RNA replication (McKnight & Lemon, 1996). Internally located sequences which are required for RNA replication have not been described within the protein-coding regions of any other picornavirus genome.

Here, we show that the HRV-14 *cre* maps to a 96-nt sequence located within RNA encoding the amino terminal segment of the capsid protein VP1. In addition, we show that *cre* function is dependent upon formation of a stable stem-loop structure within the positive-strand RNA. Our observations suggest that this structure interacts with RNA in the 3′ noncoding segment of the genome, resulting in a complex tertiary RNA structure that is required for initiation of minus-strand RNA synthesis. These findings illustrate a heretofore unrecognized aspect of picornavirus replication that may have broad significance for the replication mechanisms of other positive-strand RNA viruses.

RESULTS

Deletion analysis of the HRV-14 genome defines a minimal sequence with *cre* activity

The subgenomic RNA ΔP1Luc (Fig. 1) contains the luciferase reporter protein coding sequence placed in frame and in lieu of all but the last 21 nt of the P1 segment of the HRV-14 genome (McKnight & Lemon, 1996). It does not undergo efficient replication following transfection into normally permissive cells. However, we previously demonstrated that the replication competence of ΔP1Luc could be restored by inclusion of a large RNA segment (nt 2117–3196) that represents the 3′ third of the HRV-14 P1 region (McKnight & Lemon, 1996). Replicon and P1-deletion mutant RNAs without this RNA segment did not replicate in transfected cells, as determined by a sensitive ribonuclease protection assay. These nonreplicating RNAs could not be rescued by superinfection with wild-type helper virus or by providing capsid proteins expressed *in trans* following cotransfection with a suitable expression vector (McKnight & Lemon, 1996, and unpubl. data). Thus, the 3′ P1 segment is involved in RNA replication and contains a *cis*-acting replication element.

To determine the minimal *cre* sequence which supports HRV-14 RNA replication, we carried out an extensive mutational analysis. We assessed the replication competence of subgenomic HRV-14 RNAs containing a nested series of in-frame deletions within the implicated P1 segment (Fig. 2A). These mutants were constructed within the background of the ΔP1Luc/VP3 replicon that contains nt 2117–3196 of the P1 region downstream of the luciferase coding sequence. This RNA replicates efficiently following its transfection into permissive cells (see Fig. 1; McKnight & Lemon, 1996). We monitored luciferase activity present at 24 h following transfection of these different deletion mutants (Fig. 2A), because it is a good measure of the replication competence of such RNAs (Andino et al., 1993; Van Kuppeveld et al., 1995; McKnight & Lemon, 1996). In each experiment, the nonreplicating ΔP1Luc RNA served as a negative control and produced an average luciferase activity of only 100–200 light units (Fig. 2B). This minimal amount of luciferase activity probably reflects the translational activity of the input-transfected RNA. In contrast, the replication-competent ΔP1Luc/VP3 always produced over 100-fold greater amounts of luciferase activity by 24 h following transfection. With the exception of ΔP1Luc/VP3Δ2504, each of these deletion mutants expressed substantially greater levels of luciferase than did the negative control ΔP1Luc, indicating amplification of the transfected RNAs (Fig. 2B). As shown, there was significant, but reproducible, variation in the luciferase activities expressed following transfection of these successfully replicating RNAs. This is likely to be due to variably efficient processing of the luciferase-VP3-VP1 or luciferase-VP1 fusion proteins by the *trans* activity of the $3CD^{pro}$ viral proteinase. The variable lengths of polyprotein that remain fused to the COOH-terminus of the luciferase proteins expressed from these RNAs may also influence their enzymatic activity. Variation in the specific activity of the expressed luciferase proteins was strongly indicated by the fact that there was little difference in the replication competence of these RNAs observed in ribonuclease protection assays (see Fig. 2C)[1]. In contrast to the other deletion mutants, ΔP1Luc/VP3Δ2504 produced levels of luciferase no greater than ΔP1Luc, indicating that it failed to undergo RNA replication (Fig. 2B).

The replication phenotypes of each of the seven deletion mutants shown in Figure 2A were independently confirmed by ribonuclease protection assay following transfection of the RNA transcripts. As shown in Figure 2C, each of the deletion mutants except ΔP1Luc/VP1Δ2504 was efficiently amplified within 24 h of

[1]We have previously shown that a synthetic $3CD^{pro}$ cleavage site engineered at the end of the luciferase sequence in ΔP1Luc/VP3 is efficiently utilized *in trans* by the viral proteinase (McKnight & Lemon, 1996). However, this synthetic site may be too close to the natural VP1-VP3 cleavage site in /VP1Δ2252 for recognition by the proteinase, thus leaving a 22-amino-acid sequence fused to the COOH terminus of luciferase expressed from this construct. ΔP1Luc/VP1 contains the natural VP3-VP1 cleavage site preceded by three Gly residues in an attempt to provide flexibility at the luciferase-VP1 cleavage site.

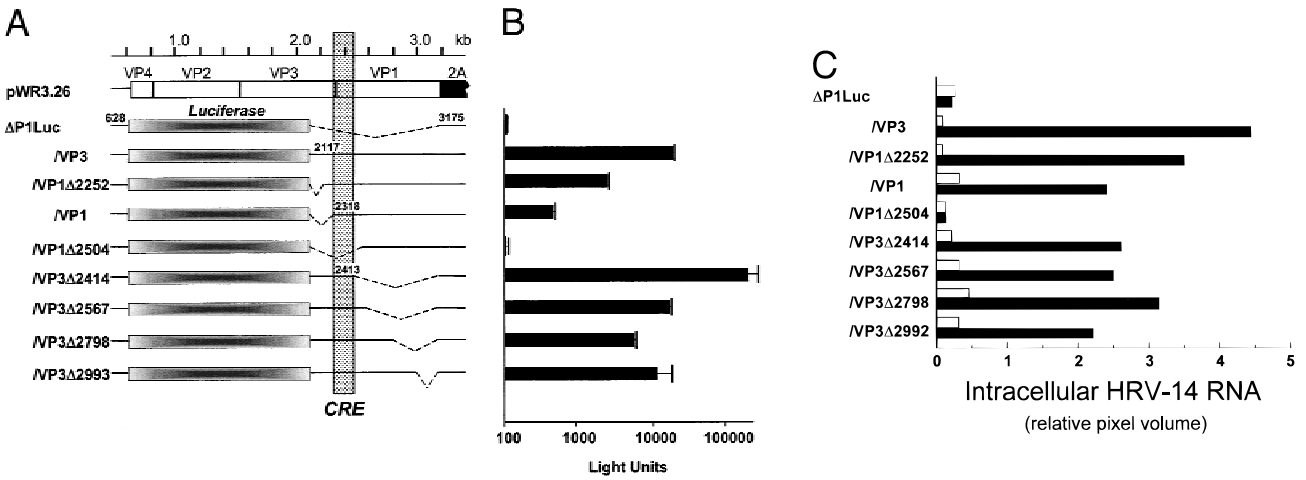

FIGURE 2. Deletion analysis of the ΔP1Luc/VP3 replicon reveals a minimal *cre* sequence. **A**: P1 deletion mutants constructed in the background of ΔP1Luc/VP3 (see Fig. 1). A schematic for the intact P1 segment in pWR3.26 and the nonviable *cre*-deficient replicon ΔP1Luc are shown for comparison. The dashed lines indicate the additional sequence deleted from the P1 segment in each of the mutants (ΔP1Luc/VP1Δ2252: nt 2117–2252, /VP1: nt 2117–2317, /Δ2504: nt 2117–2504, /Δ2414: nt 2414–3175, /Δ2567: nt 2567–3175, /Δ2798: nt 2798–3175, and /Δ2993: nt 2993–3175). The stippled box indicates the minimal *cre* segment identified in this experiment. See Materials and Methods for complete details of the deletion constructions. **B**: Luciferase activity derived from duplicate RNA transfections in H1-HeLa cells for each deletion construct and controls (ΔP1Luc and ΔP1Luc/VP3) at 24 h following transfection. The error bars indicate the range between two independent transfections. **C:** Amplification of viral RNA following transfection of P1-deleted replicon RNAs confirms the minimal active *cre* sequence. At 0 (open column) and 24 (solid column) h post-transfection, total cell lysates were analyzed for levels of viral RNA by ribonuclease protection assay with an antisense probe corresponding to the junction of the 3B and 3C gene regions. Protected RNA fragments were separated on a 6% urea–polyacrylamide gel, and specific bands were quantitated by a Molecular Dynamics PhosphorImager. For each lysate hybridized, a glyceraldehyde-3-phosphate dehydrogenase (GAPDH) cellular control probe was included (USB), with protected GAPDH fragments quantitated as above. Intracellular HRV RNA is reported as a ratio representing the volume of pixels for the viral probe divided by the volume of pixels for the protected GAPDH fragments. Pixel volume is equivalent to d.p.m.

transfection. Protected RNA fragments were generally comparable in quantity to those produced by ΔP1Luc/VP3, as determined by PhosphorImager analysis. As expected from analysis of luciferase activities in transfected cells, there was no increase in the abundance of the protected RNA fragment in cells transfected with either ΔP1Luc/VP1Δ2504 or the replication-defective ΔP1Luc transcript. Thus, the ribonuclease protection assay confirmed the results of the luciferase assays described above. Each of the replication-competent RNAs shares a 96-nt segment of a common P1 sequence located between nt 2318 and 2413, or that part of the P1 segment encoding the amino terminus of VP1.

Re-insertion of the minimal *cre* sequence in ΔP1Luc restores RNA replication

We next determined whether we could restore RNA replication competence to ΔP1Luc RNA by re-inserting the minimal *cre* sequence defined in the above experiments. First, we modified the ΔP1Luc plasmid so that it contained two new unique restriction sites located at the 3′ end of the luciferase coding sequence. This was accomplished without disrupting the integrity of the reading frame (see Material and Methods). As shown in Figure 3B, the transfection of RNA derived from this modified plasmid, ΔP1LucXN, resulted in no more luciferase activity than that obtained with ΔP1Luc, which meant it also remained incapable of replication. A PCR-amplified cDNA fragment representing nt 2318–2413 was then inserted in frame at the newly created restriction sites to produce the plasmid pΔP1Luc$_{CRE}$ (Fig. 3A). The amount of luciferase expressed from this plasmid (ΔP1Luc$_{CRE}$) was comparable to that following transfection with the replication-competent ΔP1Luc/VP3 (Fig. 3B). Thus, the insertion of the previously defined minimal *cre* sequence (nt 2318–2413; Fig. 2) had clearly restored replication competence to ΔP1Luc. PCR fragments which represented 26-nt (ΔP1Luc$_{CRE}$d2) or 56-nt (ΔP1Luc$_{CRE}$d1) fragments of this minimal sequence were also inserted into ΔP1LucXN (Fig. 3A). However, no comparable increase in luciferase activity was observed following transfection of these RNAs, and thus they remained defective for replication (Fig. 3B). These results indicate that the length of the minimal functional *cre* is between 67 and 96 nt.

The extent to which the RNAs shown in Figure 3A undergo replication was confirmed by a ribonuclease protection assay (Fig. 3C). As expected, cell lysates collected over the 24-h period following transfection of ΔP1Luc$_{CRE}$ RNA contained increasing HRV-14 RNA levels equivalent to those present following transfection of ΔP1Luc/VP3 RNA (Fig. 3C). In contrast, there was little

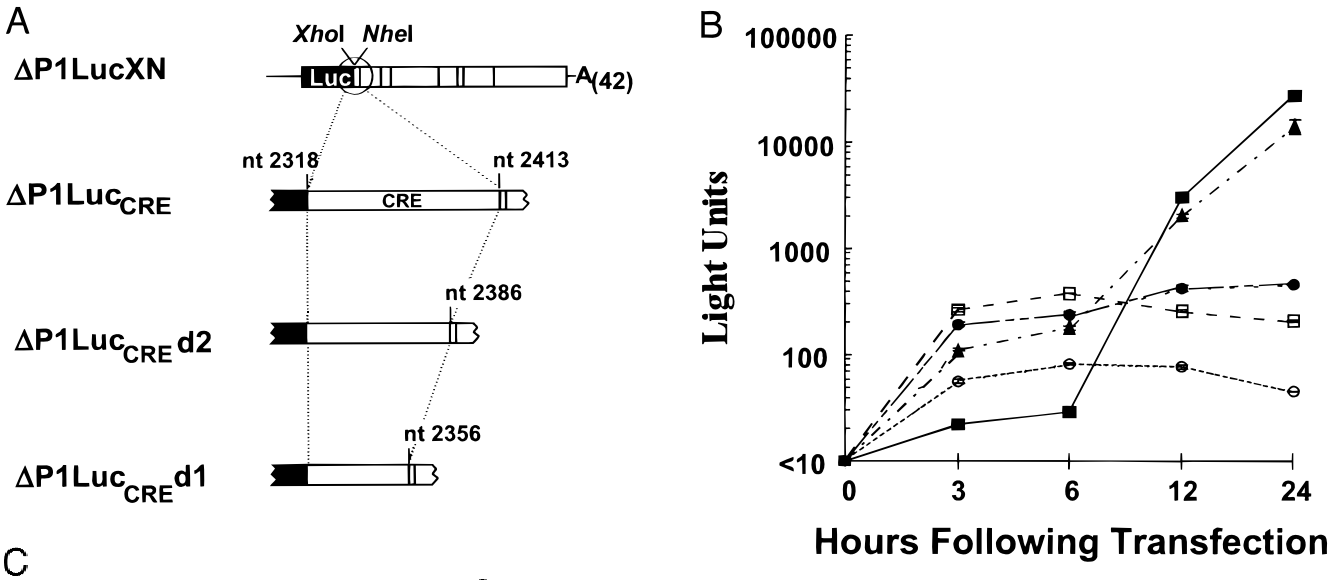

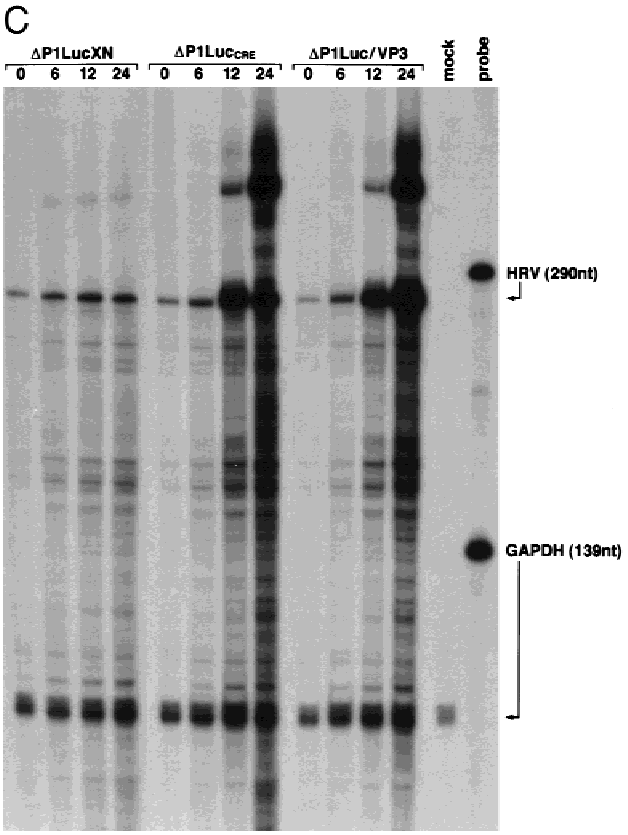

FIGURE 3. Re-insertion of the minimal *cre* sequence restores replication competence to ΔP1Luc. **A**: The modified *cre*-deficient ΔP1LucXN RNA is shown with the two engineered restriction sites, *Xho*I and *Nhe*I, placed immediately downstream of the luciferase-coding sequence (Luc; see Materials and Methods). Expanded views indicate the insertion of the minimal *cre* sequence spanning nt 2318–2414 at these sites in ΔP1LucXN to create the ΔP1Luc$_{CRE}$ replicon. Similar insertions representing smaller fragments of the minimal *cre* resulted in ΔP1Luc$_{CRE}$d1 and ΔP1Luc$_{CRE}$d2. **B**: Luciferase activity from cell lysates following transfection of the indicated replicon RNAs into H1-HeLa cells. Shown are the enzyme activities produced from transfection of ΔP1Luc/VP3 (solid box), ΔP1LucXN (open box), ΔP1Luc$_{CRE}$ (triangle), ΔP1Luc$_{CRE}$d1 (solid circle), and ΔP1Luc$_{CRE}$d2 (open circle) at 0, 3, 6, 12, and 24 h following transfection. **C**: Ribonuclease protection assay of total cell lysates prepared at the indicated times following transfection of H1-HeLa cells. Virus-specific RNA produced following the transfection of the indicated replicon RNA was detected in lysates by hybridization with an HRV-specific probe (HRV) followed by RNase treatment and PAGE as described in Materials and Methods. As in Fig. 2C, the internal control probe (GAPDH) allowed monitoring of the cellular RNA content of each lysate. Protected fragments that are specific for virus (263 nt) and for GAPDH (100 nt) are indicated by arrows. "Mock" represents a lysate of mock transfected cells. The "probe" lane contains an aliquot of each probe representing 1/100th of the quantity used in each hybridization reaction. The higher molecular weight material that is HRV probe-specific and present only in the replicating samples likely represents protected RNA hybrids which escaped the denaturation conditions of the gel (data not shown).

or no increase in HRV-14 RNA after transfection of ΔP1LucXN, or ΔP1Luc$_{CRE}$d2 and ΔP1Luc$_{CRE}$d1 (data not shown), indicating failure of RNA replication (Fig. 3C).

Dicistronic RNAs with variable expression of *cre*-encoded protein indicate that the *cre* functions as an RNA element

To ascertain whether the *cre* functions as an RNA element or a protein-coding sequence, we analyzed *cre* function in a dicistronic virus background in which it was possible to dissociate RNA replication and translation. Molla et al. (1992) obtained a viable dicistronic viral genome after insertion of the encephalomyocarditis virus (EMCV) internal ribosomal entry site sequence (IRES) into the open reading frame of poliovirus at the P1-P2 junction. Proteins from this virus are produced by proteolytic processing of two distinct polyproteins or cistrons, P1 and P2-P3, which specify the capsid proteins and nonstructural proteins, respectively. We constructed a similar dicistronic HRV-14 ge-

nome, pWREP23, by inserting the EMCV IRES at the P1-P2 junction as indicated in Figure 4. The upstream or first cistron, under the normal translational control of the HRV-14 IRES, coded for the P1 region (capsid proteins) and terminated with a stop codon after the penultimate Tyr codon of VP1. The downstream or second cistron, under control of the EMCV IRES, included the first 15 nt of the EMCV ORF (nt 260–848). Its translation initiated at an AUG-codon fused to the 3′ 21 nt of the VP1 sequence that encodes the COOH-terminal 7 amino acids of P1, leading to expression of the P2 and P3 nonstructural proteins (see Fig. 4). The sequences flanking the EMCV insert were purposefully modified to reduce the probability of loss of the segment through homologous recombination (see Materials and Methods and Fig. 4).

Compared to wild-type virus (WR3.26), virus rescued from the WREP23 dicistronic RNA had a small plaque phenotype (Fig. 4), which indicated the insertion of the EMCV IRES had interfered with some step in HRV-14 replication. A similar observation was made with dicistronic poliovirus (Molla et al., 1992, 1993). The specific infectivity of WREP23 RNA was 9.85×10^5 pfu/μg compared to 8.4×10^6 for the parental WR3.26 virus. Thus, the WREP23 RNA was viable, but produced smaller plaques with a specific infectivity that was almost tenfold less than that of synthetic wild-type RNA. The WREP23 RNA was not completely stable, but the EMCV IRES was not lost from the genome until after 5–6 virus passages (data not shown).

This novel dicistronic rhinovirus RNA provided a valuable tool with which we could address *cre* function during the initial rounds of replication that follow transfection of synthetic RNA. Because of its dicistronic nature, translation of the *cre*-containing P1 RNA could be dissociated from translation of the replicative (nonstructural) proteins encoded by the P2-P3 segment by creating a stop codon within P1. Accordingly, within the genetic background of pWREP23, we constructed several candidate dicistronic replicons as shown in Figure 5A. pΔP1LucEP23 contained the luciferase-coding sequence in the first cistron, replacing the 5′ two-thirds of the P1 sequence of pWREP23 and fused to nt 2117 of the P1 segment via a synthetic $3CD^{pro}$ cleavage site at its 3′ end. Thus, the 5′ terminus and upstream cistron of this dicistronic replicon is similar to that of the replication-competent pΔP1Luc/VP3 replicon that contains the *cre* (Fig. 1).

pΔP1LucSEP23, a second candidate dicistronic replicon, also contained the luciferase coding sequence in the first cistron, but with no HRV-14 P1 sequences (and thus no *cre*; see Fig. 5A). In both pΔP1LucEP23 and

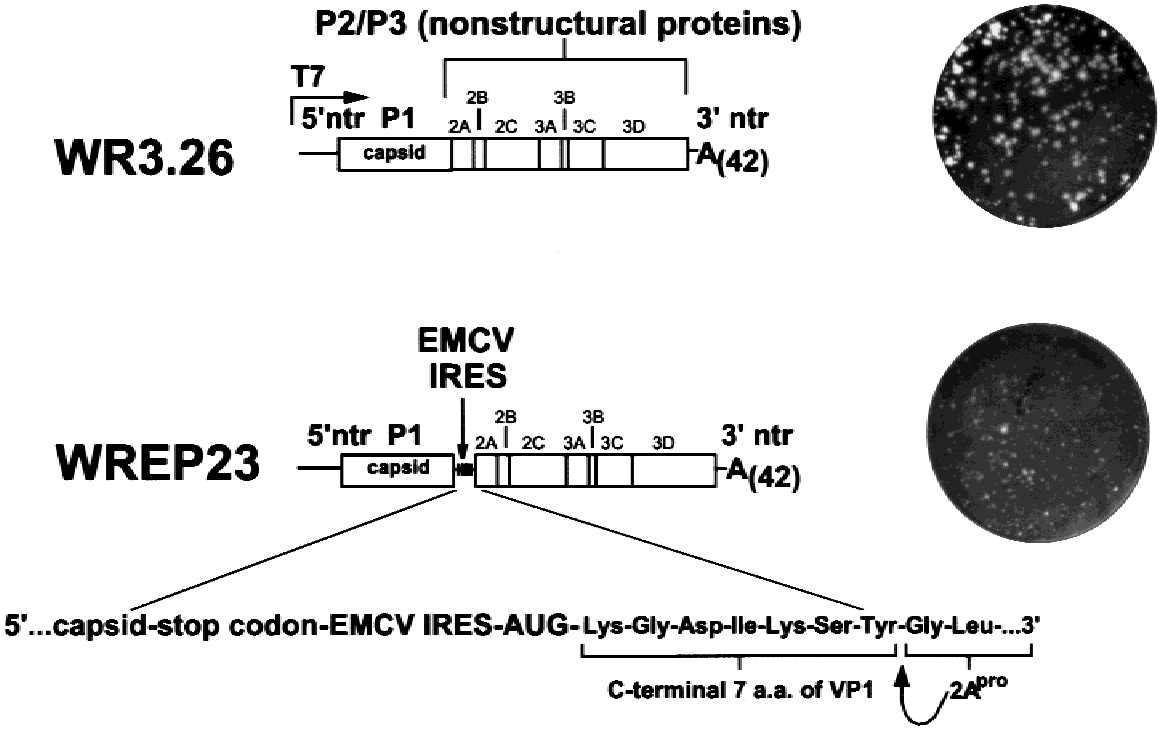

FIGURE 4. Genetic organization and plaque assay of the dicistronic HRV-14 virus rescued from pWREP23. At the top is the wild-type genome and plaques visualized at 48 h following transfection in H1-HeLa cells. Immediately below is the schematic representation of the dicistronic genome and plaques visualized following its transfection. Note that the third positions of the codons for the 7 C terminal amino acids of VP1, which are required in the upstream cistron to maintain proper $2A^{pro}$ cleavage, were altered from wild type to reduce the potential for recombination with the cognate downstream sequence.

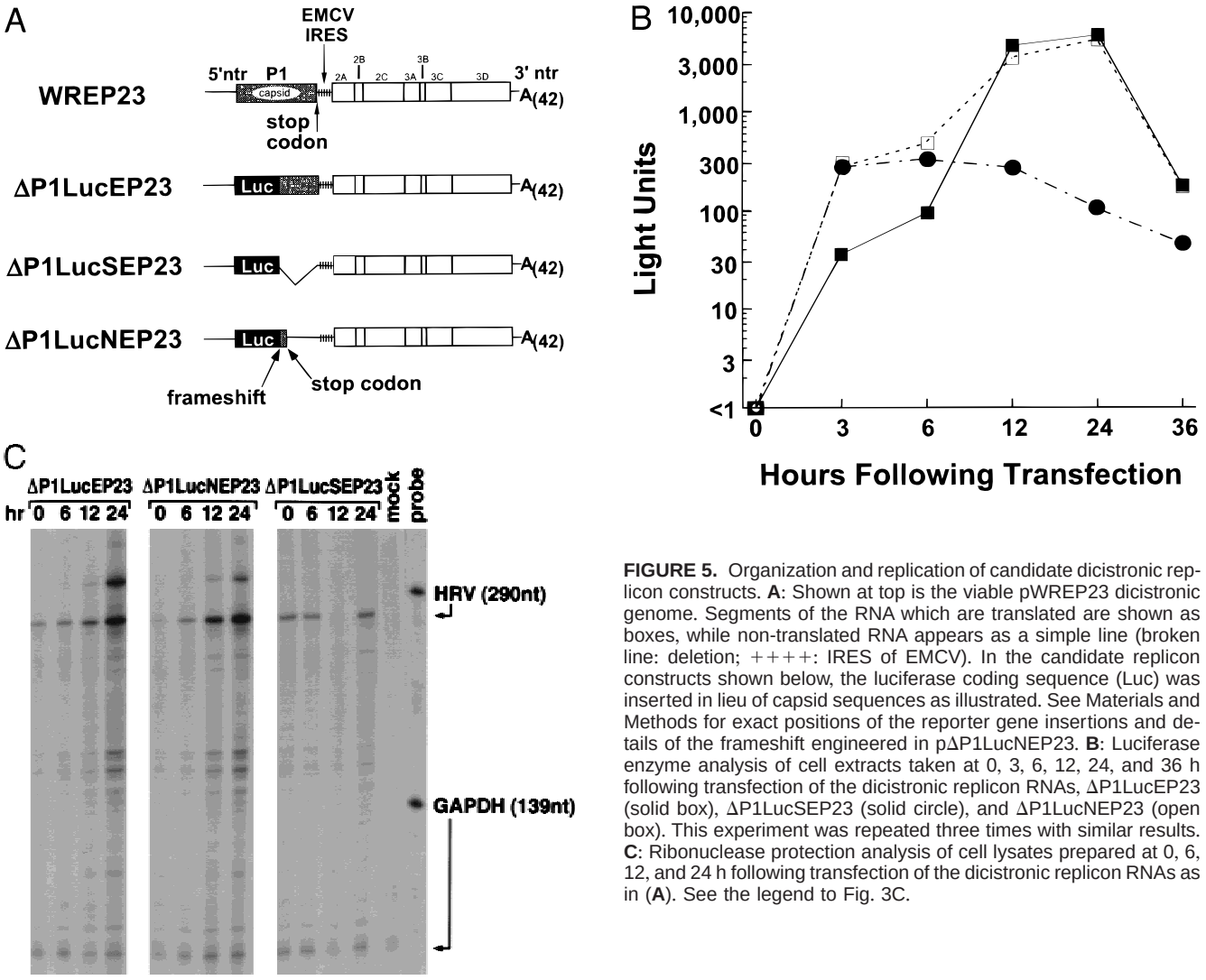

FIGURE 5. Organization and replication of candidate dicistronic replicon constructs. **A**: Shown at top is the viable pWREP23 dicistronic genome. Segments of the RNA which are translated are shown as boxes, while non-translated RNA appears as a simple line (broken line: deletion; ++++: IRES of EMCV). In the candidate replicon constructs shown below, the luciferase coding sequence (Luc) was inserted in lieu of capsid sequences as illustrated. See Materials and Methods for exact positions of the reporter gene insertions and details of the frameshift engineered in pΔP1LucNEP23. **B**: Luciferase enzyme analysis of cell extracts taken at 0, 3, 6, 12, 24, and 36 h following transfection of the dicistronic replicon RNAs, ΔP1LucEP23 (solid box), ΔP1LucSEP23 (solid circle), and ΔP1LucNEP23 (open box). This experiment was repeated three times with similar results. **C**: Ribonuclease protection analysis of cell lysates prepared at 0, 6, 12, and 24 h following transfection of the dicistronic replicon RNAs as in (**A**). See the legend to Fig. 3C.

pΔP1LucSEP23, the open reading frame present within the first cistron terminated with a stop codon placed immediately upstream of the EMCV IRES. A third dicistronic replicon, pΔP1LucNEP23, was constructed by creating a frameshift mutation upstream of the previously defined minimal *cre* segment within the first cistron of ΔP1LucEP23. This resulted in a new stop codon located 21 nt into the P1 sequence downstream of luciferase (Fig. 5A). Thus, ΔP1LucNEP23 contained the *cre* RNA sequence, but in a context which did not permit its translation into protein. Importantly, the short length of P1 sequence upstream of the stop codon in the first cistron of ΔP1LucNEP23 was shown in previous experiments (Figs. 2 and 3) to be neither necessary nor sufficient for *cre* function.

Increasing amounts of luciferase were produced following the transfection of ΔP1LucEP23 RNA, indicating that this dicistronic RNA which contains the *cre* was replication competent (Fig. 5B). As expected, transfection of the *cre*$^{(-)}$ ΔP1LucSEP23 RNA resulted in expression of only minimal luciferase activity, consistent with translation of the input RNA only. Interestingly, luciferase expression following transfection with ΔP1LucNEP23 RNA (which contained the *cre* sequence in a context which did not allow its translation), indicated a level of replication similar to that of the replication competent ΔP1LucEP23. Increases in luciferase levels indicative of efficient RNA replication were observed within 12 to 24 h following transfection. Ribonuclease protection assays confirmed that both ΔP1LucEP23 RNA (in which the *cre* is present and translated) and ΔP1LucNEP23 (*cre* present but not translated) were able to replicate. With both RNAs, increasing amounts of protected RNA fragments were documented in lysates collected over the 24 h after transfection (Fig. 5C). In contrast, there was no amplification of RNA in cells transfected with ΔP1LucSEP23 RNA (no *cre*; Fig. 5C). Thus, while the *cre* is essential for efficient HRV-14 RNA replication, it is not necessary for this short sequence to undergo translation. These

unexpected results indicate that the *cre* acts as an RNA element, and not through an expressed protein product.

It is interesting that the ΔP1LucNEP23 RNA reproducibly produced higher luciferase activity than ΔP1LucEP23 RNA at early time points following transfection (compare luciferase levels at 3 and 6 h following transfection in Fig. 5B). This increase may be due to the shorter length of the upstream cistron in ΔP1LucNEP23 compared to ΔP1LucEP23 (Fig. 5A). Alternatively, since luciferase is expressed from ΔP1LucEP23 as a fusion with ΔVP3-VP1, its activity depends on processing *in trans* by $3CD^{pro}$, whereas the first cistron of ΔP1LucNEP23 expresses luciferase fused to only seven amino acids of VP3. Thus, the difference in luciferase activities at these early time points might reflect a delay in expression of adequate levels of $3CD^{pro}$ by ΔP1LucEP23.

The function of the *cre* is dependent upon the formation of structure within the positive-strand HRV-14 RNA

The MFOLD program (see Materials and Methods) predicts that the minimal *cre* sequence comprising nt 2318–2413 of the HRV-14 genome may adopt stable secondary structures in either the positive-strand or minus-strand forms of the viral RNA (Fig. 6). Such structures could be important for RNA–RNA or RNA–protein

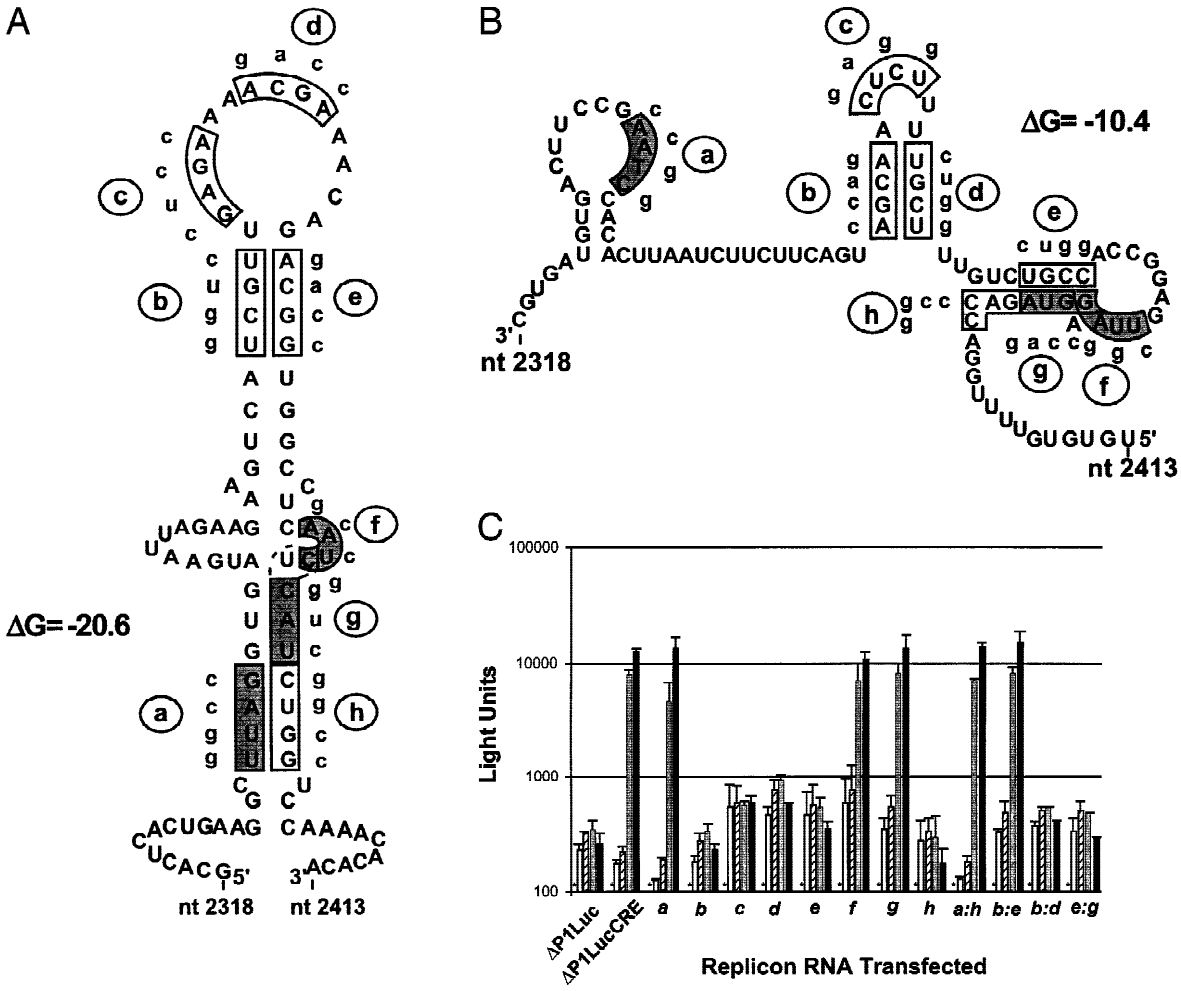

FIGURE 6. Secondary structure of the minimal *cre*. Using the MFOLD program (Genetics Computer Group, University of Wisconsin) with the folding temperature set at 34 °C and the remaining parameters set at default, the minimal *cre* sequence spanning from nt 2318–2414 of the HRV-14 genome was analyzed for the optimal predicted secondary structure formed by the **(A)** positive- or **(B)** minus-strand RNA. The predicted free energies for these structures are indicated. Note that the minus-strand structure is presented in the 3′ to 5′ direction. For mutations *a* to *h*, the 4-nt block substitution is indicated with the substituted nucleotides shown in lower case. The shaded blocks represent the mutations that were viable. Details of the nucleotide substitutions and the strategy used to create these mutants are described in Materials and Methods. **C**: Luciferase expression as a measure of replication of *cre* mutants following transfection in H1-HeLa cells. At 0 (*), 3 (open column), 6 (striped), 12 (shaded), and 24 (solid) h following transfection of the mutant RNA, lysates were harvested and analyzed for luciferase content as described in Materials and Methods. The results are an average of two independent transfections with error bars indicating the range. The luciferase activities at 0 h (*) were all less than 0.01 light units.

interactions required for replication of HRV-14 RNA. In an effort to confirm the existence of these structures and to determine whether either of the putative positive-strand or minus-strand structures are required for *cre* function, we employed site-directed mutagenesis to alter the nucleotide sequence within the *cre*. Six of the mutations we created (Fig. 6, mutations *a*, *b*, *d*, *e*, *g*, and *h*) consisted of an in-frame, 4-nt substitution, which was predicted to disrupt base pairing in either or both of the predicted positive- or minus-strand structures. Selected pairs of these mutations were covariant in that they were designed to restore base-pair interactions that were predicted to be disrupted by single mutations. Since the predicted regions of helical structure differ in the positive- and minus-strand RNAs (Fig. 6), this approach seemed likely to identify the form of RNA in which the *cre* is active. Thus, in the positive-strand RNA, mutations *a:h* and *b:e* were complementary and predicted to restore base pairing, while this was the case for mutations *b:d*, and *e:g* in the minus-strand RNA. In addition, two other mutations (Fig. 6, *c* and *f*) were created that altered the *cre* sequence in regions predicted to be entirely or largely single-stranded in either form of the RNA.

These mutated CREs were inserted in the replication-competent ΔP1LucCRE replicon, and luciferase activities were monitored following RNA transfection into H1-HeLa cells. Results are shown in Figure 6C. The single mutations *a*, *f* and *g* did not impair the replication competence of the RNA as determined by the level of luciferase expression, whereas each of the remaining five single mutations, *b*, *c*, *d*, *e*, and *h*, disrupted *cre* function and replication, as evidenced by the lack of luciferase expression above that directed by the input RNA. Although both *b* and *e* were lethal to replication when present as single mutations within the replicon RNA, the combination of *b:e* dramatically restored replication competence to the replicon RNA, resulting in a level of luciferase expression comparable to that of the replicon containing wild-type *cre* sequence (Fig. 6C). Similarly, although *h* was lethal as a single mutation, the double mutant *a:h* replicated efficiently, meaning that replication competence could be restored to *h* by the presence of the compensatory *a* mutation.

Since the *a:h* and *b:e* combinations restore base pairing within the predicted positive-strand *cre* structure (but not in the predicted minus-strand structure, Fig. 6), these data provide evidence for both the existence of the positive-strand structure, as well as its role as a functional element that is required for efficient RNA replication. In contrast, the combinations of mutations *b:d* and *e:g*, both of which are predicted to restore base-pairing within the putative minus-strand structure that would have been disrupted by the lethal single mutations, were nonviable and did not give rise to luciferase expression above that directed by the input RNA (Fig. 6C). Thus, site-directed mutagenesis confirmed the existence of structure within the positive-strand *cre* sequence, but not the minus-strand *cre* sequence. The results of these experiments indicate that the *cre* functions within the context of positive-strand RNA.

It is noteworthy that both the single *a* and *g* mutations did not interfere with *cre* function, although both alter the sequence within the proximal helical segment of the predicted positive-strand structure (Fig. 6). Although this may be taken as evidence that this lower stem is not essential for *cre* function, the lethal nature of the *h* mutation and its rescue by *a* in the viable *a:h* double mutant argue strongly against this interpretation of the results. It is more likely that the single *a* and *g* mutations allow formation of alternative helical structures involving these segments of the RNA which are permissive for *cre* function. Indeed, MFOLD predictions of these mutant sequences suggest that this may be the case (data not shown). An additional mutant, *i*, in which a different 4-nt substitution was created at the same site as in mutation *a* (Fig. 6), failed to replicate (data not shown). These results provide further evidence that the proximal helix of the predicted positive-strand structure is required for efficient replication and also serves to further map the 5′ limits of the *cre* to nt 2331–2335. At a minimum, however, the viability of the *a* and *g* mutants points to the potential plasticity of the base of the positive-strand structure as well as the lack of a need for conservation in the primary sequence of the bulge loop that separates the two major helical segments of this extended structure. That the primary sequence within the 3′ bulge loop is not essential is also indicated by the viability of mutant *f* (Fig. 6C).

In contrast, however, the lethal effects of mutations *c* and *d* on RNA replication (Fig. 6C) suggest that primary sequence within the top loop of this structure may be critically important for replication. The lethal effect of *d* is unlikely to be related to its ability to disrupt a putative stem-loop in the minus-strand RNA (Fig. 6B), because lethality was not reversed by combination with the compensating *b* mutation. However, further experiments will be required to more precisely determine the requirement for conservation of this top-loop sequence.

The *cre* is essential for initiation of minus-strand RNA synthesis

The dependence of *cre* function upon structure within the positive-strand RNA, as shown in the experiments depicted in Figure 6, suggests (but does not prove) that it may play a role in the synthesis of minus-strand RNA. To test this hypothesis, we directly compared the synthesis of minus-strand RNA in cells transfected with the replication-defective ΔP1Luc RNA (which lacks the *cre*) and the replication-competent ΔP1Luc/VP3 RNA, using a modified two-cycle ribonuclease protection assay originally described for poliovirus (Novak & Kirkegaard,

1991; Fig. 7A). This method is reported to allow direct quantitation of poliovirus minus-strand RNA with a 100-fold increase in sensitivity compared to the standard ribonuclease assay (femtomoles of RNA were easily detected; Novak & Kirkegaard, 1991). However, this experimental approach is complicated because the accumulation of minus-strand RNA ultimately depends upon positive-strand RNA synthesis, because new progeny positive-strand molecules serve as a template for additional minus-strand synthesis. Nonetheless, our previous studies document that increases in positive-strand HRV-14 RNA do not occur until more than 3 h following transfection of synthetic RNA into H1-HeLa cells (McKnight & Lemon, 1996). Thus, any minus-strand RNA detected within 3 h of transfection is almost certainly produced by transcription of the input RNA. As shown in Figure 7A, no minus-strand RNA could be detected in lysates from cells transfected with ΔP1Luc RNA at this point in time, even on longer exposure of the gel. In contrast, in cells transfected with ΔP1Luc/VP3 RNA, minus-strand RNA was readily detected as a faint band in the 3-h sample. The quantity of minus-strand RNA increased over the 24 h following transfection of ΔP1Luc/VP3, but minus-strand RNA was never observed in cells transfected with RNA lacking the *cre*. To confirm these findings, we compared the synthesis of minus-strand RNA in cells transfected with the ΔP1Luc and ΔP1Luc/VP3 RNAs using a combination of ribonuclease protection and rTth reverse transcription (RT)-PCR. We developed this two-stage procedure because RNA isolated from transfected H1-HeLa cells contains significant quantities of the input positive-strand RNA (Fig. 3C; McKnight & Lemon, 1996). Furthermore, excessive amounts of viral positive-strand RNA can lead to false detection of minus-strand RNA, even with putatively strand-specific RT-PCR assays (Lanford et al., 1994, 1995). To avoid this, we removed excess positive-strand RNA by RNase treatment after hybridizing all available minus-strand RNAs to positive strands (Novak & Kirkegaard, 1991). Equimolar amounts of positive and minus strands are obtained by this procedure, increasing the specificity of minus-strand RNA detection. After ribonuclease treatment, we subjected the protected RNAs to rTth RT-PCR, a method shown to provide 10,000- to 100,000-fold specificity for detection of the correct strands in assays of synthetic positive- and minus-strand RNAs (Lanford et al., 1994; 1995).

Using this approach, no minus-strand RNA could be detected in lysates from cells transfected with ΔP1Luc RNA at 3, 6, or 24 h following transfection (Fig. 7B, lanes 1, 4, and 7). Similarly, transfection of a replicon that encodes a defective polymerase (ΔP1Luc/VP3$^{(-pol)}$; McKnight & Lemon, 1996) also failed to produce minus-strand RNA detectable by this method (Fig. 7B, lanes 3, 6, and 9). In contrast, minus-strand RNA could

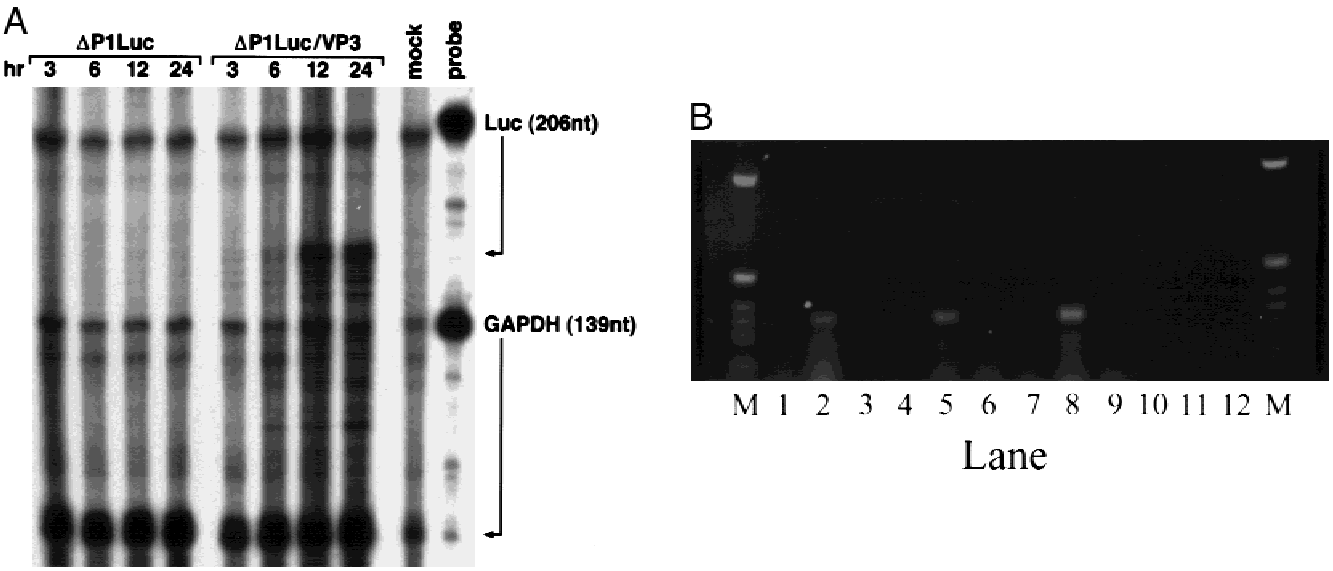

FIGURE 7. Analysis of replicon minus-strand RNA synthesis. **A**: A two-cycle ribonuclease protection assay was carried out as described in Materials and Methods on total cell lysates prepared at the indicated times following transfection. The nonspecific bands in each sample are likely a result of second-cycle hybridization between probe and probe DNA template that had escaped the RQ1 DNase treatment. The legend is as for Figure 3C. **B**: H1-Hela cells transfected with ΔP1Luc, ΔP1Luc/VP3, and ΔP1Luc/VP3$^{(-pol)}$ replicon RNAs and subjected to ribonuclease protection and RT-PCR as described in Materials and Methods. Lanes 1–3 represent samples isolated at 3 h following transfection, lanes 4–6 at 6 h, and lanes 7–9 at 24 h. cDNA synthesis and PCR of ΔP1Luc is shown in lanes 1, 4, and 7; ΔP1Luc/VP3 in lanes 2, 5, and 8; and ΔP1Luc/VP3$^{(-pol)}$ in lanes 3, 6, and 9. Lane 10 is RNA isolated from mock-transfected H1-HeLa cells. Lane 11 is a no-reverse transcription control of the ΔP1Luc/VP3 RNA at 24 h and lane 12 is a water only, no template control. M: 1 kb DNA ladder (Life Sciences, Inc.).

be easily detected within 3 h of transfection of the replication-competent ΔP1Luc/VP3 RNA (Fig. 7B, lane 2). The quantity of minus-strand RNA increased substantially over the 24 h following transfection of ΔP1Luc/VP3 (Fig 7B, lanes 5 and 8), as expected. These results are consistent with the *cre* having a role in minus-strand RNA synthesis.

DISCUSSION

Here we have shown that HRV-14 genome contains a novel, internally located *cre* that is between 83 and 96 nt in length. Although located within a protein-coding segment of the genome, the *cre* function is independent of its translation (Fig. 5B,C). Thus, this segment of the viral RNA has dual functions, both encoding the VP1 capsid protein and participating directly in the replication of the viral genome. A detailed mutational analysis (Fig. 6) confirmed the existence of a computer-predicted RNA structure within the positive-strand *cre* sequence, and further demonstrated that this structure is required for replication. These data indicate that the *cre* functions within the context of the positive-strand RNA. Because we were unable to document the production of minus-strand RNA from HRV-14 RNAs that lack the *cre* (Fig. 7), this *cre* appears to be required for initiation of minus-strand RNA synthesis.

Similar internally located *cre* have never been described in other picornaviruses. Unlike the situation with HRV-14, replicon RNAs derived from other picornaviruses (poliovirus or coxsackievirus B3) replicate efficiently despite the absence of all or almost all of the P1 capsid protein-coding segment (Andino et al., 1993; Porter et al., 1995; Van Kuppeveld et al., 1995). Borman et al. (1994) suggested the existence of essential RNA replication signal(s) within sequence located several hundred nucleotides from the 5′ end of the poliovirus genome, within the nontranslated RNA comprising the IRES segment. However, strong doubt has been cast on this conclusion by the work of Lu & Wimmer (1996), who were able to construct viable poliovirus chimeras in which the hepatitis C virus IRES completely replaced the poliovirus IRES (and the putative replication signals). All other reported picornaviral replication signals are located within 150 nt of the 5′ or 3′ terminus of the RNA (excluding the 3′ poly-A sequence).

Nonetheless, there are no data that would exclude the presence of *cre*-like elements within the P2 or P3 coding regions of poliovirus and other picornaviruses. The proteins encoded by these segments of the genome appear to function primarily *in cis* with respect to the replication of RNA (Wimmer et al., 1993; Novak & Kirkegaard, 1994). While a few P2-P3 mutants have been found to be *trans*-complementable, the *cis*-acting nature of these proteins makes it difficult if not impossible to identify such an RNA replication element.

Despite the apparent novelty of the HRV-14 *cre* among picornaviruses, *cis*-acting replication signals have been identified within the genomes of other positive-strand viruses. These include the plant pathogen brome mosaic virus (BMV; Pogue & Hall, 1992) and the bacteriophage Qβ (Barrera et al., 1993). In addition, a replication signal has been identified within the internal, protein-coding segment of the genomic RNA of some strains of the coronavirus mouse hepatitis virus (MHV) (Kim & Makino, 1995; Luytjes et al., 1996). Similarly, a *cis*-acting, internally located RNA sequence has been suggested to be required for replication of the RNA of flock house virus (Ball & Li, 1993). This latter virus has a distant evolutionary relationship to HRV-14 and other picornaviruses. However, its putative replication signal is not well characterized and it is thus difficult to compare it with the HRV-14 *cre*. It is not clear that any of these other internally located replication signals function in a fashion similar to that of the HRV-14 *cre*. Indeed, the MHV replication signal is required for positive-, and not minus-strand RNA synthesis (Kim & Makino, 1995). However, the presence of such elements within a wide range of positive-strand RNA virus families suggests a possible common theme in the replication of these agents.

The precise mechanism by which the HRV-14 *cre* contributes to RNA replication remains to be defined, but several possibilities may be envisioned. The requirement for preservation of the positive-strand *cre* structure (Fig. 6) suggests that this segment of the RNA may serve as a recognition site for viral or cellular proteins involved in the replication process. However, the fact that the HRV-14 3′ ncr can be completely deleted and still produces viable virus (Todd et al., 1997) points to a certain degree of flexibility in this model. It may be that in the absence of the 3′ ncr a cryptic structure is formed, perhaps in conjunction with the polyA tail, that allows formation of a replicase recognition site. The important conclusion that is suggested by our findings here is that the global folding of internal RNA segments may strongly influence the ability of a viral RNA to replicate. Kim & Makino (1995) suggested, but did not formally prove, the importance of internal RNA structure in the replication of mouse hepatitis virus RNAs. This may be a general attribute of positive-strand viruses, albeit one that may be difficult to prove in individual cases because the RNA possesses overlapping protein-coding functions.

Pogue et al. (1994) suggested that the internally located signals in BMV replicative intermediates could serve as recognition sites for a helicase complex of cellular or viral origin. They envisioned that this interaction might initiate the separation of positive- and minus-strands of the double-stranded RNA, freeing the end of a particular strand for initiation of subsequent rounds of RNA synthesis. In this model, at least one round of minus-strand RNA synthesis would

occur in the absence of the internal replication signal. Since a sensitive two-cycle ribonuclease protection and a coupled ribonuclease protection:RT-PCR assay were both unable to detect minus-strand RNA synthesis from a replicon lacking the *cre* (Fig. 7), this model appears untenable for HRV-14 *cre* function. As an alternative, Pogue et al. (1994) as well as Barrera et al. (1993) suggested that internal replication signals might act as a site for replicase assembly, possibly in conjunction with 5′ or 3′ terminal sequences. In such a role, the internal replication signal could function to guide the replicase complex to the specific site of strand initiation. This model for *cre* function is very attractive, because it is consistent with the data presented.

Either an essential role in directing an RNA–protein interaction or involvement in a tertiary RNA structure required for viral RNA synthesis could suggest that the distance between the *cre* and the 5′ or 3′ end of the viral RNA might be critical. However, this does not appear to be the case. A previously constructed, replication-competent HRV-14 deletion mutant (CAPd2) contained a 1366-nt deletion upstream of the *cre*, which placed the *cre* within 123 nt of the 5′ nontranslated RNA (McKnight & Lemon, 1996). In addition, the replication-competent ΔP1Luc/VP3Δ2414 mutant contains a downstream deletion which brings the *cre* 761 nt closer to the 3′ end of the genome (Fig. 2). Thus the exact distance between the *cre* and either the 5′ or 3′ end of the genome is not of critical importance. Furthermore, these results suggest that local sequence may largely define the proper folding of the *cre*.

Tertiary RNA structures involving loop–loop interactions within the 3′ terminal sequences of other picornaviruses (poliovirus and coxsackievirus A9) play an essential role in the initiation of minus-strand RNA synthesis (Jacobson et al., 1993; Pilipenko et al., 1996; Mirmomeni et al., 1997). These structures appear necessary for efficient assembly of the replicase complex at the 3′ end of the positive-strand RNA, but are not absolutely required for replication (Todd et al., 1997). Perhaps significantly, the 3′ terminal RNA sequence of HRV-14 is less structured than the comparable segments of poliovirus or coxsackievirus RNA (Todd & Semler, 1996). Thus it is possible the *cre* may act as a surrogate for 3′-terminal structures present in other picornaviruses but lacking in HRV-14 (e.g., the most 5′ stem-loop of the highly structured 3′ terminus of poliovirus RNA; Pilipenko et al., 1996). According to this model, the *cre*, in interacting with the 3′ end of HRV-14 RNA, would serve as a site for replicase assembly, guiding the replicase complex to the site of minus-strand initiation. Such a model is consistent with the absence of detectable minus-strand RNA synthesis from HRV-14 RNAs which lack the *cre* (Fig. 7). It is also consistent with the presence of minimal essential *cis*-acting sequences at the 3′ end of flock house virus RNA, which has been suggested to contain an internal *cre* (Ball & Li, 1993; Ball, 1994).

MATERIALS AND METHODS

Cells

H1-HeLa cells were obtained from the American Type Culture Collection and maintained in 1× MEM supplemented with Earles' salts (Gibco/BRL), L-glutamine, and 10% fetal calf serum.

Virus

HRV-14 was recovered following transfection of H1-HeLa cells with RNA transcribed from the infectious cDNA clone pWR3.26 (Lee et al., 1993; McKnight & Lemon, 1996). Plaque assay of HRV-14 on H1-HeLa cell monolayers was carried out as previously described (Sherry & Rueckert, 1985). For passaging of the dicistronic virus, both cells and supernatant from a 60-mm plate were harvested together 24 h following transfection and subjected to three rounds of freezing and thawing in an Eppendorf tube. The resulting lysate was clarified by microcentrifugation and frozen at −70 °C as a virus stock. For further passaging, fresh H1-HeLa cells in a 35-mm dish were infected using 250 μL of virus stock. The resulting infected cells were harvested as above.

Construction of *cre*$^{(-)}$ and dicistronic RNAs and *cre* mutants

Deletions of the capsid-coding region containing the *cre* were accomplished in the background of pΔP1Luc/VP3. The construction of this plasmid has been described previously (McKnight & Lemon, 1996), and involved fusion of the luciferase coding sequence to a synthetic 3CD^{pro} cleavage site, and its insertion in-frame in lieu of nt 629-2116 of the P1 coding sequence. Further deletions of the residual capsid coding sequence were as follows.

(a) pΔP1Luc/VP1Δ2252

Using the PCR primers 5′-GTA*CCATGG*ataagtgcatgtccag-3′ (where the underlined bases represent a *Nco*I) and 5′-cctgttgagactattgc-3′, a fragment spanning nt 2252–3313 of the HRV-14 genome was produced from pWR3.26 cDNA. This PCR product was digested with *Nco*I and *Arv*II (nt 3206 of HRV-14) and ligated to the sites in the subclone pSPHRVluc/VP3 (McKnight & Lemon, 1996). A *Cla*I to *Avr*II fragment was excised from this subclone and ligated to pΔP1Luc/VP3, producing a replicon with a deletion of 129 nt between the Trp codon at nt 2123 and the Ile codon ending at nt 2252 (Fig. 2).

(b) pΔP1Luc/VP1

A DNA fragment was amplified from pΔP1Luc/VP3 with the following primers: 5′-cgatgacttcttctaattcatcacctaagccttcagtga gtgcGCCGCCGCC**caatttggactttccgc**-3′ (where the bold face bases are luciferase coding sequence) and 5-**ggcgcacctctttt**

cgaaagaagtcggg-3′ (primer 1). A second PCR fragment was generated with following set of primers: 5′-**gagagatcctcata aaggccaagaagggcggaaagtccaaattg**GGCGGCGGCgcactc actgaaggcttaggtg-3′ and 5′-cccaccgtacctaggtcctaaacc-3′ (primer 2). One microliter each of the above PCR products was gel purified and used as a template in an overlap extension PCR with primer 1 and primer 2. The PCR fragment was digested with *Cla*I and *Dra*III and ligated to the sites in pΔP1Luc/VP3. The resulting deletion removes the 201 nt of capsid-coding sequences extending from the Pro codon at nt 2117 to the Ala codon beginning at nt 2318.

(c) pΔP1Luc/VP1Δ2504

The primer 5′-ctacctacatg*CCTAGG*cactttaatggttcag-3′ and primer 2 were used in a PCR with pWR3.26 as a template. The resulting product was digested with *Nco*I and *Avr*II and ligated to the sites in pSPHRVluc/VP3. The small *Cla*I to *Dra*III fragment was removed from this subclone and ligated to the sites in pΔP1Luc/VP3. This deletion removes the 384 nt of capsid-coding sequence between the Pro codon at nt 2120 and the His codon at nt 2504 of the HRV-14 genome.

(d) pΔP1Luc/VP3Δ2414

The primer 5′-gat*CCTAGG*tcctaaaccATAGGATTTAATGTCA CCTTTtgtgtgttttggaccag-3′ was used in a PCR with primer 1 and pΔP1Luc/VP3 as a template. The resulting fragment was digested with *Cla*I and *Avr*II (italicized bases) and ligated to the sites in pΔP1Luc/VP3. This deletion removes the 762 nt of capsid-coding sequence between the Thr codon beginning at nt 2414 and the Lys codon beginning at nt 3176, and retains the 7 C-terminal amino acids of VP1 (capitalized above) to allow proper $2A^{pro}$ cleavage.

(e) pΔP1Luc/VP3Δ2567

The primer 5′-gat*CCTAGG*tcctaaaccATAGGATTTAATGTC ACCTTTtacatgcacacaagctgc-3′ was used in a PCR with primer 1 and pΔP1Luc/VP3 as a template. The resulting fragment was digested with *Cla*I and *Avr*II (italicized) and ligated to the sites in pΔP1Luc/VP3. This deletion removes the 609 nt of capsid-coding sequence between the Val codon at nt 2567 and the Lys codon at nt 3176, as in pΔP1Luc/VP3Δ2413.

(f) pΔP1Luc/VP3Δ2798

Two micrograms each of the linker-primers 5′-gtgccaaaggtg acattaaatcctatggtttaggac-3′ and 5′-ctaggtcctaaaccataggattt aatgtcacctttggcaccag-3′ were mixed together in 5 μL ligase buffer, incubated at 65 °C for 10 min, and slow-cooled to room temperature. The linker formed by this reaction contains *Dra*III (nt 2795 of the HRV-14 genome) and *Avr*II (nt 3206) overhangs, and was ligated to the *Dra*III and *Avr*II sites in pΔP1Luc/VP3, producing a 378-nt deletion from the Val codon that ends at nt 2798 to the Lys codon beginning at nt 3176.

(g) pΔP1Luc/VP3Δ2993

The linker-primers 5′-tatgaaaggtgacattaaatcctatggtttaggac-3′ and 5′-ctaggtcctaaaccataggatttaatgtcacctttca-3 were annealed as described above, and ligated to the *Nde*I (nt 2989) and *Avr*II sites in pΔP1Luc/VP3, producing a 183-nt deletion that extends from the Met codon at nt 2993 to the Lys codon at nt 3176.

Construction of an HRV-14 replicon containing the minimal *cre* sequence

In PCR 1, primer 3, (5′-ggatttaatgtcacctttt*GCTAGC*ccc*CTC GAG***caatttggactttcc**-3′) and primer 1 were used in a standard PCR with ΔP1Luc as a template. The resulting 716-nt product was digested with *Cla*I and *Xho*I. PCR 2 utilized ΔP1Luc as a template, primer 4 (5′-**ggaaagtccaaattg***CTC GAG*ggg*GCTAGC*aaaggtgacattaaatcc-3′) and the primer 5′-gatttggtcagtgaacccg-3′ to generate a 509-nt PCR product extending to nt 3679. This product was digested with *Xho*I and *Pvu*II (nt 3569 of HRV-14) and subcloned into the *Xho*I and *Nae*I of Bluescript KS+ vector (Stratagene), to produce the subclone pBSLXNsc. This plasmid was digested with *Cla*I and *Xho*I and ligated to the similarly digested product of PCR 1 to produce pBSLXN. A *Cla*I to *Avr*II fragment was removed from pBSLXN and ligated to the unique sites of ΔP1Luc to produce ΔP1LucXN (Fig. 3A).

DNA fragments representing candidate minimal *cre* sequences (Fig. 3A) were generated by PCR for subcloning into ΔP1LucXN. The return primer for three different reactions was primer 5, 5′-cagactgtt*CTCGAG*gcactcactgaaggc-3′, which incorporates a *Xho*I site immediately before nt 2318 of HRV-14. The first PCR utilized the primer, 5′-caacgat *GCTAGC*gacttcttc-3′, which placed an *Nhe*I site at nt 2356 of HRV-14. A second primer, 5′-gattga*GCTAGC*ggccacc-3′, placed the *Nhe*I site at nt 2386, and a third primer 5′-ggtctttttg*GCTAGC*tgtgtgttttgg-3′ placed the *Nhe*I at nt 2413. The template for all three reactions was pWR3.26. Each PCR product was digested with *Xho*I and *Nhe*I, electrophoresed in a 1.5% Seaplaque agarose gel, and ligated to these sites in ΔP1LucXN.

Dicistronic virus and replicon constructs

An HRV-14 dicistronic virus was constructed in which the P1 and P2 junction is interrupted by the EMCV IRES (corresponding to nt 259–849 of the EMCV genome). The IRES segment was amplified by PCR from pCITE (Novagen, Inc.) using the following primers: 5′-caccgtacc**actagtaggtccta**aa ccata*cgacttgatatcgccc*ttCATGGTTGTGGCCATATTA-3′ and 5′-cggaattcc**gatatC**CCCCTCTCCCTCCC-3′ (where the lower case, nonboldface characters represent HRV-14 sequences and the capitalized bases represent EMCV sequences). In the first primer, the AUG ending at nt 848 of the EMCV genome is fused to nucleotides encoding the last seven amino acids of VP1 to retain the $2A^{pro}$ cleavage which occurs between the last residue of P1 (Tyr) and the first residue of P2 (Gly). To reduce the likelihood of homologous recombination between the 21 nt and their counterparts in the P1 region, the third positions of six of the codons were changed without altering the encoded protein sequence (italicized bases in the above primer). The PCR product was digested with *Spe*I and *Eco*RV (boldface in the primer sequences) and ligated into the plasmid pSPcap-s (pSPcap-s contains the entire HRV-14 capsid sequence, ending with a UGA stop codon followed by

the above unique sites in the pSP64 cloning vector) at the *Avr*II and *Eco*RV sites to create pSPcapEMC. pSPcapEMC was digested with *Ppu*MI (boldface in the first primer) and *Nde*I. The small fragment was isolated and ligated to pWR3.26 to create pWREP23 that contains the full-length sequence of a dicistronic HRV-14.

Candidate dicistronic replicons were constructed from pWREP23 as follows. A pSPcapEMC fragment isolated following digestion with *Aat*II and *Nco*I was fused to the luciferase gene isolated from ΔP1Luc/VP3 following *Aat*II and *Nco*I digestion, and ligated to the sites in pSPcapEMC to produce the subclone pSPLuc/VP3EP23. The small *Sal*I and *Apa*I fragment of pSPLuc/VP3EP23 was ligated to the large fragment of pWREP23 to create the replicon pΔP1LucEP23. A frameshift was introduced in pΔP1LucEP23 by linearizing the plasmid DNA 25 nt downstream of the luciferase gene (immediately following the synthetic $3CD^{pro}$ cleavage site) by digestion with *Nco*I. The linearized molecule was filled in with Klenow enzyme and re-ligated. As a result of the frameshift, a stop codon was situated 24 nt downstream of the capsid sequence contained in pΔP1LucEP23, 1053 nt upstream of the EMC IRES. The frameshift mutant was designated pΔP1LucNEP23.

Finally, using pΔP1Luc plasmid DNA with the PCR primer 5′-gccatg*gatatc*TCA**caatttggactttcccttcttggc**-3′ (boldface nucleotides represent luciferase sequences) and primer 1 above, a DNA fragment was produced which contained a stop codon (capitalized) and a unique *Eco*RV site (italicized) immediately following the luciferase gene. This fragment was digested with *Cla*I and *Eco*RV and ligated to the *Acc*I and *Sma*I sites of the pSPEMC vector (pSPEMC contains the EMC IRES from pCITE within the cloning vector pSP64), creating the subclone pSPELucstop. The small *Bse*RI fragment of pSPELucstop was ligated to pΔP1LucEP23. After screening for correct insert orientation, this dicistronic replicon was designated pΔP1LucSEP23.

Site-directed mutagenesis of the *cre* sequence

Mutations were created within the background of $p\Delta P1Luc_{CRE}$ that contains the minimal active *cre* sequence. Primers for these PCR mutagenesis reactions were as follows (nucleotide substitutions in boldface):

mutation *a* [5′-gtccaaattgctcgaggcactcactgaaggc**ggcc**gtg atg-3′],
mutation *b* [5′-gtccaaattgctcgaggcactcactgaaggctaggtgatgaa ttagaagaagt**cagg**tctgag-3′,
mutation *c* [5′-cctttgctagctgtgtgttttggaccgatgagattgaggccaccg tctgtttcgttt**ggag**aacgatg-3′],
mutation *d* [5′-cctttgctagctgtgtgttttggaccagatgagattgaggcca ccgtctgtt**ggtc**tttc-3′],
mutation *e* [5′-cctttgctagctgtgtttttggaccagatgagattgaggcca**ggtc** ctg-3′],
mutation *f* [5′-cctttgctagctgtgtgttttggaccagatga**cggc**gagg-3′],
mutation *g* [5′-cctttgctagctgtgtttttggaccag**gac**a**c**attgagg-3′],
mutation *h* [5′-cctttgctagctgtgtttttgga**ggcc**atgag-3′].

The return PCR primer for mutation *a* and *b* was primer 1 (above), and for the other mutations, primer 2. The fragments produced by the *a* and *b* PCR reactions were digested with *Xho*I and *Nhe*I and cloned directly into $p\Delta P1Luc_{CRE}$. Products from the other mutagenesis reactions were digested with *Nhe*I and *Cla*I (within the luciferase sequence), and cloned into $p\Delta P1Luc_{CRE}$ as above.

All manipulated regions of each DNA construct were sequenced. Agarose gel purifications of DNA fragments used for ligation were done using the Wizard PCR Preps procedure (Promega) or the QIAgel gel extraction procedure (Qiagen).

In vitro transcription and transfection

To produce full-length replicon or infectious RNA transcripts in vitro, 2–3 μg of the parental or recombinant cDNA-containing plasmids were linearized at the unique *Sma*I site 9 nt downstream of the viral genome. RNA transcripts were synthesized from the linear templates using T7 polymerase in a previously described 100 μL in vitro system (McKnight & Lemon, 1996). Transcript RNA was quantitated and verified by agarose gel analysis.

We prepared 5×10^6 H1-HeLa cells for each electroporation with 10–20 μg of transcript RNA, as previously described (McKnight & Lemon, 1996). Equivalent amounts of transcript RNA were used in each experiment. Electroporated cells were plated into two 60-mm dishes or four 35-mm wells of a six-well plate and cultured in DMEM with 10% FBS at 34 °C until processing of the cell monolayers for further analysis.

Analysis of luciferase enzyme activity

Transfected cells were processed for enzyme assays by the addition of 250 μL lysis buffer (Luciferase Assay Kit, Promega) per 60-mm dish. Lysates were stored at −70 °C until enzymatic analysis. Five μL of lysate (or lysate diluted 1:10 with lysis buffer) was mixed with 100 μL of luciferase substrate mixture (Promega). The samples were immediately monitored for light output using a BioOrbit model 1250 luminometer.

Ribonuclease protection assays

Ribonuclease protection assays were carried out with reagents and protocols supplied with the Lysate Ribonuclease Protection Kit (United States Biochemicals). Transfected cell monolayers in 60-mm dishes were lysed by adding 100 μL of a solution containing 4 M guanidine thiocyanate, 25 mM sodium citrate, and 0.5% sarcosyl. Lysates were stored at −70 °C until hybridization. Riboprobes for monitoring positive-strand RNA synthesis and cellular glyceraldehyde-3-phosphate dehydrogenase (GAPDH) messenger RNA were constructed and prepared as previously described (McKnight & Lemon, 1996). We added 1×10^6 cpm of each probe to 45 μL of lysate, and carried out hybridization directly in lysate solutions at 37 °C for 18 h (overnight), as described by the manufacturer. The hybridization mixture was subsequently diluted tenfold and digested with RNase and proteinase. Protected RNA fragments were separated by electrophoresis in 6% polyacrylamide–6 M urea gels and visualized by autoradiography.

Minus-strand RNA synthesis was analyzed using a modification of the two-cycle ribonuclease protection assay of Novak & Kirkegaard (1991). Using the USB reagents and protocols, overnight hybridizations with cell lysates in the first cycle contained 10^6 cpm of the GAPDH control riboprobe. After RNase and proteinase treatment, the RNAs were precipitated in isopropanol and resuspended directly in 45 μL of lysis buffer, and 10^6 cpm of a riboprobe specific for minus-strand luciferase gene sequences was added. The reactions were heated to 95 °C for 5 min, hybridized as above, and RNase treated as before. Protected RNA fragments were visualized using electrophoresis as with the positive-strand analysis. The luciferase riboprobe was generated with SP6 polymerase in vitro transcription using the plasmid pGEMLuc (Promega) as template following digestion with *Bsi*WI. The resulting riboprobe was 206 nt long, of which 153 nt represent the luciferase gene and were protected by RNase treatment following hybridization with minus-strand luciferase RNA.

Coupled ribonuclease protection and reverse transcription-PCR

At the times indicated following transfection of 5×10^6 H1-HeLa cells, total RNA was extracted and isolated using an RNA isolation kit (RNAqueous, Ambion, Inc.). RNAs were additionally purified by RQ1-DNase (Promega) treatment and LiCl precipitation to ensure removal of any contaminating replicon plasmid DNA. One half of the total purified RNA was used directly in a ribonuclease protection assay as described above, except no riboprobe was added. Following proteinase treatment, the samples were phenol-chloroform extracted and isopropanol precipitated. The resulting protected RNAs were resuspended in a 25-μL RT reaction using the rTth DNA polymerase protocol and reagents provided by the manufacturer (Promega). RNAs were first melted at 94 °C for 2 min, after which the reaction temperature was lowered to 70 °C and the polymerase and forward primer were added. The reaction temperatures were quickly lowered to 60 °C to allow forward primer annealing and then heated to 70 °C for 30 min to allow cDNA synthesis. Then, 25 μL of pre-warmed chelating buffer (2×) and return primer were added to each reaction and the temperature was increased to 94 °C for 3 min. The subsequent PCR consisted of 40 cycles at 94 °C for 30 s, 60 °C for 1 min, and 72 °C for 2 min. The forward primer for the RT and PCR reactions was [5′-cacactaagccccccaac-3′], which anneals at nt 4602 of the HRV-14 genome. The return primer for PCR was [5′-ctggaggtggtgtgttgc-3′], which anneals at nt 4951 and should result in amplification of a 366-bp DNA product. Finally, 10 μL of each PCR reaction were applied to a 1.0% agarose gel in 1× TAE buffer, and products were visualized by staining with ethidium bromide.

ACKNOWLEDGMENTS

This research was supported by grants from the National Institute of Allergy and Infectious Diseases (RO1-AI-140282) and the Cystic Fibrosis Foundation (S880). K.L.M. was supported by institutional and individual National Institutes of Health training grants (T32-AI07151 and F32-AI09984).

Received June 12, 1998; returned for revision July 27, 1998; revised manuscript received August 12, 1998

REFERENCES

Andino R, Rieckhof GE, Achacoso PL, Baltimore D. 1993. Poliovirus RNA synthesis utilizes an RNP complex formed around the 5′-end of viral RNA. *EMBO J 12*:3587–3598.

Ball LA. 1994. Replication of the genomic RNA of a positive-strand RNA animal virus from negative-sense transcripts. *Proc Natl Acad Sci USA 91*:12443–12447.

Ball LA, Yi L. 1993. cis-acting requirements for the replication of flock house virus RNA 2. *J Virol 67*:3544–3551.

Barrera I, Schuppli D, Sogo JM, Weber H. 1993. Different mechanisms of recognition of bacteriophage Qβ plus and minus strand RNAs by Qβ replicase. *J Mol Biol 232*:512–521.

Bienz K, Egger D, Troxler M, Pasamontes L, 1990. Structural organization of poliovirus RNA replication is mediated by viral proteins of the P2 genomic region. *J Virol 64*:1156–1163.

Borman AM, Deliat FG, Kean KM. 1994. Sequences within the poliovirus internal ribosome entry segment control viral RNA synthesis. *EMBO J 13*:3149–3157.

Choi WS, Pal-Ghosh R, Morrow CD. 1991. Expression of human immunodeficiency virus type 1 (HIV-1) *gag, pol,* and *env* proteins from chimeric HIV-1-poliovirus minireplicons. *J Virol 65*:2875–2883.

Cole CN. 1975. Defective interfering (DI) particles of poliovirus. *Prog Med Virol 20*:180–207.

Gwaltney JM Jr. 1995. Rhinovirus infection of the normal human airway. *Am J Respir Crit Care Med 152*:S36–S39.

Hodgman TC. 1988. A new superfamily of replicative proteins. *Nature 333*:22–23.

Jacobson SJ, Konings DA, Sarnow P. 1993. Biochemical and genetic evidence for a pseudoknot structure at the 3′ terminus of the poliovirus RNA genome and its role in viral RNA amplification. *J Virol 67*:2961–2971.

Kajigaya S, Arakawa H, Kuge S, Koi T, Imura N, Nomoto A. 1985. Isolation and characterization of defective-interfering particles of poliovirus Sabin 1 strain. *Virology 142*:307–316.

Kaplan G, Racaniello VR. 1988. Construction and characterization of poliovirus subgenomic replicons. *J Virol 62*:1687–1696.

Kim YN, Makino S. 1995. Characterization of a murine coronavirus defective interfering RNA internal cis-acting replication signal. *J Virol 69*:4963–4971.

Kuge S, Saito I, Nomoto A. 1986. Primary structure of poliovirus defective-interfering particle genomes and possible generation mechanisms of the particles. *J Mol Biol 192*:473–487.

Lanford RE, Chavez D, Chisari FV, Sureau C. 1995. Lack of detection of minus-strand hepatitis C virus RNA in peripheral blood mononuclear cells and other extrahepatic tissues by the highly strand-specific rTth reverse transcriptase PCR. *J Virol 69*:8079–8083.

Lanford RE, Sureau C, Jacob JR, White R, Fuerst TR. 1994. Demonstration of in vitro infection of chimpanzee hepatocytes with hepatitis C virus using strand-specific RT/PCR. *Virology 202*:606–614.

Lee W-M, Monroe SS, Rueckert RR. 1993. Role of maturation cleavage in infectivity of picornaviruses: Activation of an infectosome. *J Virol 67*:2110–2122.

Lu HH, Wimmer E. 1996. Poliovirus chimeras replicating under the translational control of genetic elements of hepatitis C virus reveal unusual properties of the internal ribosomal entry site of hepatitis C virus. *Proc Natl Acad Sci USA 93*:1412–1417.

Luytjes W, Gerritsma H, Spaan WJ. 1996. Replication of synthetic defective interfering RNAs derived from coronavirus mouse hepatitis virus-A59. *Virology 216:174–183.*

McKnight KL, Lemon SM. 1996. Capsid coding sequence is required for efficient replication of human rhinovirus 14 RNA. *J Virol 70*:1941–1952.

Mirmomeni M, Hughes HPJ, Stanway G. 1997. An RNA tertiary structure in the 3′ untranslated region of enteroviruses is necessary for efficient replication. *J Virol 71*:2363–2370.

Molla A, Jang SK, Paul AV, Reuer Q, Wimmer E. 1992. Cardioviral internal ribosomal entry site is functional in a genetically engineered dicistronic poliovirus. *Nature 356*:255–257.

Molla A, Paul AV, Schmid M, Jang SK, Wimmer E. 1993. Studies on dicistronic polioviruses implicate viral proteinase $2A^{pro}$ in RNA replication. *Virology 196*:739–747.

Novak JE, Kirkegaard K. 1991. Improved method for detecting poliovirus minus strands used to demonstrate specificity of positive-strand encapsidation and the ratio of positive to minus strands in infected cells. *J Virol 65*:3384–3387.

Novak JE, Kirkegaard K. 1994. Coupling between genome translation and replication in an RNA virus. *Genes & Dev 8*:1726–1737.

Paul AV, van Boom JH, Filippov D, Wimmer E. 1998. Protein-primed RNA synthesis by purified poliovirus RNA polymerase. *Nature 393*:280–284.

Percy N, Barclay WS, Sullivan M, Almond JW. 1992. A poliovirus replicon containing the chloramphenicol acetyltransferase gene can be used to study the replication and encapsidation of poliovirus RNA. *J Virol 66*:5040–5046.

Pilipenko EV, Poperechny V, Maslova SV, Melchers WJG, Bruins Slot HJ, Agol V. 1996. *Cis*-acting element, *oriR*, involved in the initiation of (−) strand poliovirus RNA: A quasi-globular multi-domain RNA structure maintained by tertiary ('kissing') interactions. *EMBO J 15*:5428–5436.

Pogue G, Huntley CC, Hall TC. 1994. Common replication strategies emerging from the study of diverse groups of positive-strand RNA viruses. *Arch Vir* (Suppl.) *9*:181–184.

Pogue G, Hall TC. 1992. The requirement for a 5′ stem-loop structure in brome mosaic virus replication supports a new model for viral positive-strand RNA initiation. *J Virol 66*:674–684.

Porter DC, Ansardi DC, Morrow CD. 1995. Encapsidation of poliovirus replicons encoding the complete human immunodeficiency virus type 1 gag gene by using a complementation system which provides the P1 capsid protein in trans. *J Virol 69*:1548–1555.

Sherry B, Rueckert RR. 1985. Evidence for at least two dominant neutralization antigens on human rhinovirus 14. *J Virol 53*:137–143.

Todd S, Semler BL. 1996. Structure-infectivity analysis of the human rhinovirus genomic RNA 3′ non-coding region. *Nucleic Acids Res 24*:2133–2142.

Todd S, Towner JS, Brown DM, Semler BL. 1997. Replication-competent picornaviruses with complete genomic RNA 3′ non-coding region deletions. *J Virol 71*:8868–8874.

Van Kuppeveld FJM, Galama JMD, Zoll J, Melchers WJG. 1995. Genetic analysis of a hydrophobic domain of coxsackie B3 virus protein 2B: A moderate degree of hydrophobicity is required for a *cis*-acting function in viral RNA synthesis. *J Virol 69*:7782–7790.

Wimmer E, Hellen CUT, Cao X. 1993. Genetics of poliovirus. *Annu Rev Genet 27*:353–436.

Xiang W-K, Paul AV, Wimmer E. 1997. RNA signals in entero- and rhinovirus genome replication. *Semin Virol 8*:256–273.